Human Molecular Genetics, 2001, Vol. 10, No. 21 2385–2396

Comparison of *Pkd1*-targeted mutants reveals that loss of polycystin-1 causes cystogenesis and bone defects

Weining Lu, Xiaohua Shen, Anna Pavlova, Montaha Lakkis, Christopher J. Ward[3], Lynn Pritchard[4], Peter C. Harris[3], David R. Genest[1], Antonio R. Perez-Atayde[2] and Jing Zhou*

Renal Division, Department of Medicine, [1]Department of Pathology, Brigham and Women's Hospital, [2]Department of Pathology, Children's Hospital, Harvard Medical School, Boston, MA 02115, USA, [3]Division of Nephrology, Mayo Clinic, Rochester, MN, USA and [4]Institute of Molecular Medicine, University of Oxford, Oxford, UK

Received June 8, 2001; Revised and accepted July 27, 2001

A high level of polycystin-1 expression is detected in kidneys of all patients with autosomal dominant polycystic kidney disease (ADPKD). Mice that overexpress polycystin-1 also develop renal cysts. Whether overexpression of polycystin-1 is necessary for cyst formation is still unclear. Here, we report the generation of a targeted mouse mutant with a *null* mutation in *Pkd1* and its phenotypic characterization in comparison with the *del34* mutants that carry a 'truncation mutation' in *Pkd1*. We show that *null* homozygotes develop the same, but more aggressive, renal and pancreatic cystic disease as *del34/del34*. Moreover, we report that both homozygous mutants develop polyhydramnios, hydrops fetalis, spina bifida occulta and osteochondrodysplasia. Heterozygotes also develop adult-onset pancreatic disease. We show further that *del34* homozygotes continue to produce mutant polycystin-1, thereby providing a possible explanation for increased immunoreactive polycystin-1 in ADPKD cyst epithelia in the context of the two-hit model. Our data demonstrate for the first time that loss of polycystin-1 leads to cyst formation and defective skeletogenesis, and indicate that polycystin-1 is critical in both epithelium and chondrocyte development.

INTRODUCTION

Autosomal dominant polycystic kidney disease (ADPKD) is one of the most common genetic diseases, characterized by the progressive replacement of renal tissue by epithelial cysts. About 50% of ADPKD patients have liver cysts (1). Pancreatic cysts are also seen (2).

Polycystins are an expanding family of a novel class of transmembrane proteins. Two members of the polycystin family (polycystin-1 and -2) are mutated in human ADPKD. Polycystin-1 is a large (~460 kDa) membrane-associated glycoprotein with a number of adhesive domains in its extracellular N-terminal region, 7–11 transmembrane domains, and a small cytoplasmic tail (3–6). Polycystin-2 (~110 kDa) is homologous to an ~400-residue hydrophobic region of polycystin-1 (7) and to voltage-activated and transient receptor potential channel subunits, which suggest that polycystins are associated with ion transport. The C-terminal tail of polycystin-1 interacts with that of polycystin-2 (8,9). Polycystin-1 signaling may be mediated by G proteins (10,11) and its signaling pathway may intersect with that of Wnts, a family of secreted signaling molecules (11). Recently, three new polycystins, polycystin-L, -L2 and -REJ, have been identified (12–14). Polycystin-L, the first polycystin whose function was determined, forms a calcium-regulated, calcium-permeable cation channel when expressed in *Xenopus* oocytes, and was proposed to function as a transducer of Ca^{2+}-mediated signaling *in vivo* (15). Very recently, it has been shown that co-assembly of polycystin-1 and -2 produces unique cation-permeable currents (16). Polycystin-2 alone also mediates cation currents and functions as a Ca^{2+}-permeable non-selective cation channel (17–19).

Polycystin-1 is widely expressed in a number of tissues and cell types (20–23), and its expression is developmentally regulated. The highest level of polycystin-1 expression is found in fetal life, while a low level of expression is maintained throughout adulthood (21,22,24). It is thus highly likely that polycystin-1 function is not only important in organs that are affected in ADPKD, i.e. kidney, liver and pancreas, but also in the development of other organs and tissues. Homozygous mutant mice with a deletion of exon 34 of *Pkd1* (*del34*, previously named *Pkd1*$^{-}$) develop severe polycystic kidney and pancreatic disease and die during the perinatal period (25). Mice heterozygous for the *del34* mutation develop late-onset polycystic kidney and liver disease (26). The *del34* mutation is a truncation mutation that mimics many mutations seen in ADPKD patients (27–29). It is

*To whom correspondence ahould be addressed at: Harvard Institutes of Medicine, Room 522, 77 Avenue Louis Pasteur, Boston, MA 02115, USA. Tel: +1 617 525 5860; Fax: +1 617 525 5861; Email: zhou@rics.bwh.harvard.edu
Present address:
Weining Lu, Genetics Division, Department of Medicine, Brigham and Women's Hospital, Boston, MA 02115, USA

unclear, however, whether such a truncation mutation results in a form of polycystin-1 with gain of function or in a 'truncated' protein that has an effect on phenotype. In humans, polycystin-1 is overexpressed in renal cystic epithelia from ADPKD patients, as shown by a number of antibodies raised against various domains of the protein (20,21,24,30–33). The rare large deletions that create *null* mutations of *PKD1* in humans are difficult to interpret (34,35) because they involve contiguous genes, including TSC2, a tuberous sclerosis gene that is independently associated with renal abnormalities such as cysts.

In the experiments described herein, we generated, by homologous recombination, a line of mice that are deficient in polycystin-1. Comparative analysis of the *null* and *del34* mice revealed that mutations in *Pkd1* result not only in epithelial defects (cyst formation) but also chondrocyte defects (osteochondrodysplasia and failure of neural arches to close). We show that polycystin-1 is present in *del34* mutants and probably partially rescues its phenotype.

RESULTS

Generation of *Pkd1 null* mutants

To study the effects of loss of polycystin-1 function in a model system, we targeted the 5′ end of the murine *Pkd1* gene by inserting a pgk-neomycin (neo) cassette into exon 4 by homologous recombination in embryonic stem (ES) cells (Fig. 1A). This insertion should result in a frame shift, generating a shortened peptide of 130 amino acids which lacks 97% of the polycystin-1 sequence. Eight recombinant ES clones were identified by Southern blot analysis with probes flanking the sequence in the targeting vector (Fig. 1B). Two independent clones (9c and h) were injected into C57BL/6 and BALB/c blastocysts, respectively. The resulting '*null*' chimaeric mice, with >80% of the agouti coat, were crossed with C57BL/6 and BALB/c mice to produce (*null*/+) F_1 progeny.

We analyzed *Pkd1* gene expression in *null* mutants by reverse-transcription polymerase chain reaction (RT–PCR) of a *Pkd1* transcript, using two sets of primers located in exons 2 and 5 (Fig. 1A). Both sets of primers revealed a mutant transcript in mRNA from *null* homozygotes and heterozygotes (Fig. 1C). DNA sequencing of this mutant transcript revealed that part of the pgk-neo cassette was spliced into the mutant *Pkd1* transcript, resulting in a stop codon 30 bp downstream of exon 3 (Fig. 1H).

Northern blot analysis of mRNA from embryonic day 12.5 (E12.5) *null* embryos with both 5′ and 3′ cDNA probes revealed a mutant transcript similar in size to that in wild-type (14 kb) *Pkd1* mRNA. The mutant transcripts were expressed at a slightly lower level in homozygotes and heterozygotes after normalization with GAPDH expression (Fig. 1D). To determine whether these mutant transcripts produce stable *Pkd1* protein, we performed western blot analysis with a monoclonal antibody 7e12 (36), directed against the extracellular N-terminal region of polycystin-1. A strong immunoreactive band of ~460 kDa was detected in wild-type and heterozygous embryos and absent in homozygous *null* mutants (Fig. 1F).

Differential expression of *Pkd1* gene in *null* and *del34* mutants

To investigate whether a mutant polycystin-1 is present in the *del34* mutants (25), expression of both *Pkd1* transcript and protein was examined in *del34* homozygotes and heterozygotes and compared with that of wild-type littermates. While *del34* homozygotes and heterozygotes continue to express large (~14 kb) mutant *Pkd1* transcripts at a reduced intensity compared with wild-type (Fig. 1E), an ~11 kb transcript was detected in *del34* homozygotes and heterozygotes by a 5′ *Pkd1* probe (Fig. 1E). This transcript was not detected by the extreme 3′ cDNA probe kg8 (data not shown).

While *null* homozygotes do not produce any detectable polycystin-1, antibody 7e12 detected a smaller band (~400 kDa) and a nearly full-length protein in *del34* heterozygotes and homozygotes by western analysis (Fig. 1G). While the nature of the nearly full length protein is unknown, the smaller protein is coincident in size to the predicted size of the truncated protein produced by the *del34* mutants, which truncates the polycystin-1 peptide by 836 residues (25).

Rapid progression of polycystic kidney and pancreatic disease in homozygous *null* embryos

Timed pregnancies were generated to analyze *null* homozygous fetuses at various developmental stages. A total of 378 mouse embryos (218 in C57BL/6-129 and 160 in BALB/c-129 background) from E12.5 to the neonatal period were isolated (Table 1). Embryos older than E15.5 were grossly examined for their kidney size, and cystic lesions in their pancreas and liver, as well as the size of their heart and lungs. A total of 17 *null* homozygotes (from E12.5 onwards) were examined histologically for renal cystic lesions. To our surprise, kidney development in *null* mutants appears to proceed normally until E15.5, when cystic dilatation of renal tubules first becomes evident (Fig. 2A). This is the same stage at which cyst formation is observed in *del34* embryos, thus indicating that polycystin-1 is required for tubular maturation but not for the initial stages of nephrogenesis, at least in the mouse strains investigated (Fig. 2B). As in *del34* mutants, lectin-binding experiments in *null* animals revealed that proximal tubules dilated prior to collecting tubules.

Null mutants seem to have larger and more renal cysts than *del34* mutants at the same stage (Fig. 2E–F). Some strain dependence in the degree of cystic lesions in mice of a given mutation was noted. Kidney lesions in BALB/c-129 background appear to be milder than that in C57/BL-129 background at the same stage, and are similar between *null* mutants of newborn stage in BALB/c-129 background (Fig. 2E) and those at E17.5 in C57BL/6-129 background (Fig. 2C). This finding suggests a moderate strain dependence on renal disease severity. The rate of cyst development indicates a more aggressive disease in homozygous *null* kidneys than in *del34* homozygotes of the same genetic background (Fig. 2A–F), thus providing the first evidence that the nature of mutation has an impact on disease progression.

The onset of pancreatic phenotype in *null* homozygous embryos was at E13.5 (i.e. at the same stage as in *del34* mutants), but the dilatation of pancreatic ducts progressed much more rapidly in *null* mutants (Fig. 2G–J).

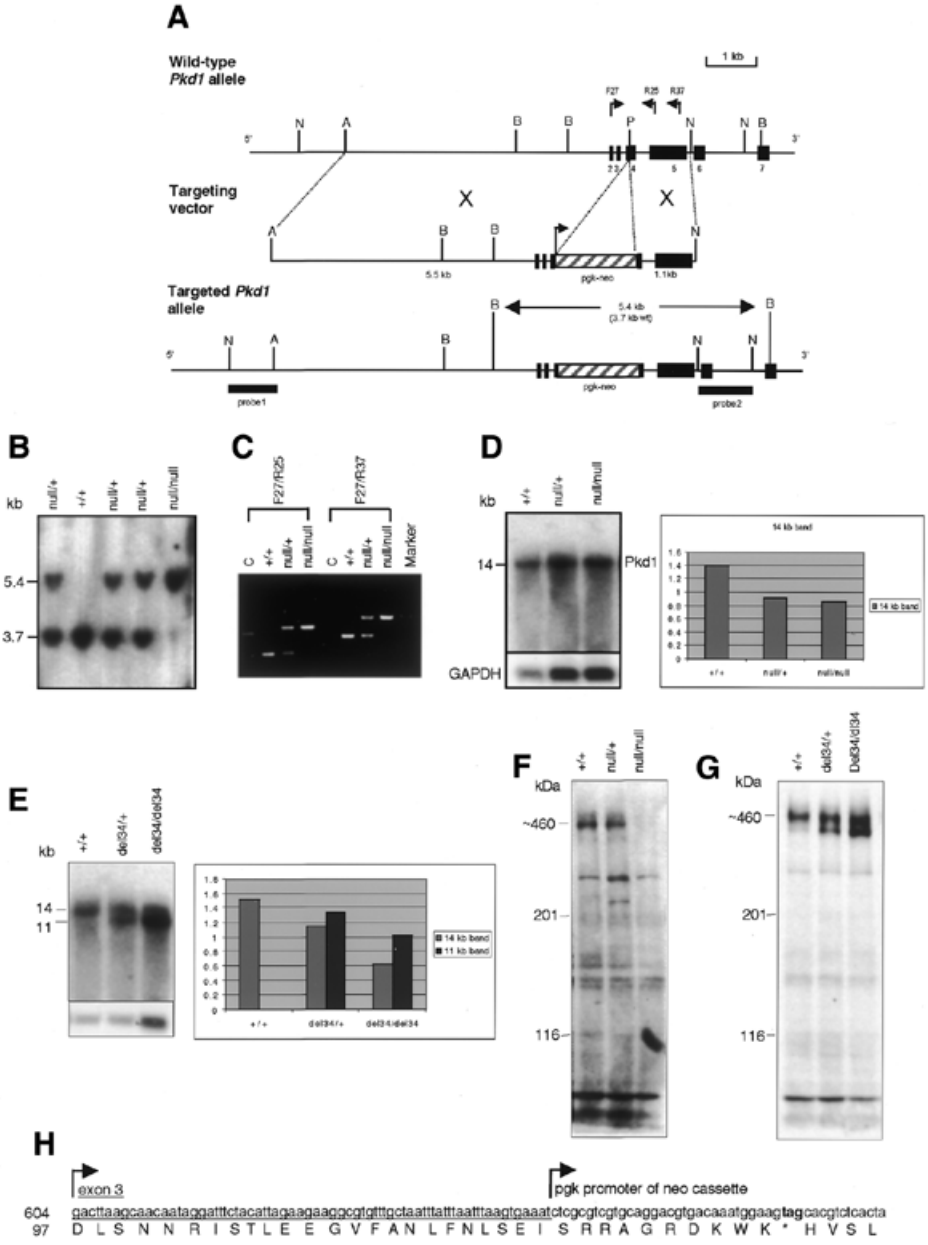

Figure 1. Targeted disruption of exon 4 of *Pkd1* and differential expression of *Pkd1* in *null* and *del34* mutants. (**A**) Structures of wild-type and targeted *Pkd1 null* alleles. A phosphoglycerate kinase (pgk) promoter-driven neo-resistant gene was inserted into exon 4 of *Pkd1*. Single arrows indicate the direction of transcription. A, *Avr*II; B, *Bam*HI; N, *Nsi*I; P, *Pml*I. F27, R25 and R37 are primers used to detect transcripts shown in (C). (**B**) Southern analysis of targeted mouse mutants. DNA isolated from F_2 *null* littermates was digested with *Bam*HI and hybridized with a 1 kb genomic fragment [probe 2 in (A), see Materials and Methods for probe 1 information]. The 3.7 and 5.4 kb bands correspond to wild-type and mutant alleles, respectively. (**C**) RT–PCR of *Pkd1* transcripts in the wild-type (+/+), heterozygous (*null*/+) and homozygous (*null/null*) whole mouse embryos using primers F27, R25 and R37, whose positions are shown in (A). C, wild-type control without reverse transcriptase. The band shown in C is an amplification product of wild-type genomic DNA (containing introns 2, 3 and 4) which is larger than the cDNA shown in the (+/+) lane. (**D**) Northern analysis of mRNA from E12.5 whole embryos was probed with a *Pkd1* cDNA probe (exons 2–6). An ~14 kb *Pkd1* transcript in wild-type (+/+), heterozygous (*null*/+), and homozygous (*null/null*) embryos was seen. A mouse glyceraldehyde 3-phosphate dehydrogenase (GAPDH) probe was used as a loading control. The intensity of the 14 kb band in all genotypes after normalization with GAPDH is shown in a chart on the right. (**E**) Northern analysis of mRNA from E12.5 whole mouse embryos. The same *Pkd1* cDNA probe used in (D) detects a full-length 14 kb *Pkd1* transcript in *del34* mutants and in wild-type. An additional 11 kb transcript was detected in *del34* heterozygotes and in *del34* homozygotes. Mouse GAPDH was used as a loading control. The intensity of the 11 and 14 kb bands in all genotypes after normalization with GAPDH is shown in a chart on the right. (**F**) Western analysis of membrane fractions from E12.5 whole mouse embryos. A monoclonal antibody (7e12) against the N-terminus of polycystin-1 detects a prominent ~460 kDa band in wild-type (+/+) and heterozygotes (*null*/+) and is absent in the homozygous (*null/null*) mutants. (**G**) Western analysis of E16.5 whole mouse embryos with the same polycystin-1 antibody used in (F), 7e12. An ~460 kDa protein (polycystin-1) was detected in wild-type and *del34* heterozygotes. A smaller band, and a nearly full-length band is overexpressed in heterozygotes and homozygotes compared with wild-type. (**H**) DNA sequence of the RT–PCR products from *null* homozygotes (C). The mutant transcript would result in a premature stop codon (tag) immediately beyond exon 3 whose sequence is underlined.

Table 1. Number of embryos examined from *Pkd1*$^{null/+}$ intercrosses at various developmental stages

Embryonic day	Total embryos (C57BL/6-129)	*null/null* (C57BL/6-129)	Dead *null/null* (C57BL/6-129)	Total embryos (BALB/c-129)	*null/null* (BALB/c-129)	Dead *null/null* (BALB/c-129)
E12.5	32	9 (1)	0	54	10 (1)	0
E13.5	28	5 (1)	0	–	–	–
E14.5	26	10 (1)	3	13	3 (1)	2
E15.5	49	11 (2)	5	27	7 (2)	5
E16.5	28	9 (2)	3	11	2 (2)	1
E17.5	32	7 (1)	6	6	1 (1)	1
E18.5	23	6	6	21	5 (2)	2

Numbers in parenthesis indicate *null* homozygotes that have been examined histologically for renal cystic lesions. All embryos >E15.5 were grossly examined for the size of their heart, kidney and lungs, and the size and visibility of cysts in their kidney, pancreas and liver.

Table 2. Kidney and liver cystic lesions in *Pkd1*$^{null/+}$ mice

	Identification no.						
	1922	1921	1938	1940	1925	1901	925
Age (months)	2.5	2.5	4	4.5	6	9	13.5
Renal cysts[a]	2	30	4	14	2	3	6
	Identification no.						
	2411	611	1932	1958	1943	925	987
Age (months)	11	11.5	13	13	13	13.5	14
Liver cysts[b]	1	1	2	2	>30	4	>30

[a]Microscopic renal cysts found in seven out of 10 mice at 2–24 months of age.
[b]Macroscopic liver cysts found in 12 out of 25 mice at 2.5–16 months of age.

Kidney, liver and pancreatic cystic disease in *Pkd1*-targeted heterozygous mice

Among 40 *null* heterozygotes (2–24 months) examined, microscopic kidney cysts were found as early as 2.5 months; in contrast *del34* heterozygotes develop scattered microscopic renal cysts at 9 months of age (26). Serial sections of kidneys from 10 *null* heterozygotes (2.5–14.5 months) revealed 2–30 cysts in seven (70%) mice (Table 2). Five out of 40 *null* heterozygotes developed visible renal cysts (at 13, 19.5, 21, 22.5 and 23 months old); three out of five had bilateral cysts.

Liver cysts are the most common extra-renal manifestation of ADPKD, occurring in ~75% of ADPKD patients aged over 60 (1). Despite the lack of discernible liver defects in *null* homozygotes, 12 out of 25 (48%) *null* heterozygotes (2.5–16 months) examined developed visible liver cysts, first observed at the age of 11 months (Table 2), similar in timing to that in *del34* heterozygotes. All 15 (100%) older *null* heterozygous mice (18–24 months) had liver cysts. Six wild-type littermates (11.5–23 months) had no cystic lesions in the liver.

Although we did not observe pancreatic cysts in 23 *del34*/+ heterozygotes (9–20 months), one out of 21 *null* heterozygotes >12 months (14.5 months) developed a single visible pancreatic cyst. Further study of a large population of old *del34*/+ mutants (>20 months) revealed that three out of 30 (10%) heterozygotes (at 22, 24 and 25 months, respectively) had macroscopic pancreatic cysts (Fig. 3A), whilst five aged-matched wild-type littermates showed no pancreatic cysts. There is no significant difference in terms of age of onset and severity of pancreatic cystic disease between theses two lines of *Pkd1* mutants. Histology showed dilatation of pancreatic ducts (Fig. 3B) and multiple cystic structures lined by cuboidal cyst epithelium (Fig. 3C). Some cysts with small lumens also contained cuboidal epithelium, with a large portion of eosinophilic cytoplasm suggesting an acinar origin (Fig. 3D). Cystic lesions were surrounded by interstitial fibrosis with few atrophic acini and isolated islets of Langerhans (Fig. 3E). Pancreatic lipomatosis was noted in areas with extensive adipose tissue replacement (Fig. 3F). This constellation of findings, including cystic disease, fibrosis and lipomatosis, is identical to that observed in patients with cystic fibrosis (37).

Pkd1 null mutation causes embryonic lethality, polyhydramnios and hydrops fetalis

Homozygous *null* embryos were found dead as early as E13.5, 2 days earlier than *del34* homozygotes with a peak around E14.5 and E16.5. Only five out of 143 homozygotes survived to term but died immediately after birth. All five were of BALB/c-129 genetic background. In the C57BL/6-129 background, all *null* homozygous embryos succumbed by E17.5, 2 days earlier than their *del34* counterparts.

Polyhydramnios was the first abnormality observed in the *Pkd1* homozygous fetus, found in *null/null* embryos as early as E12.5 (Fig. 4A and B). It was followed by systemic edema of the whole embryo (hydrops fetalis) starting at E13.5 (Fig. 4C), consistent with a sequential association found in human fetuses (38,39). Polyhydramnios and hydrops fetalis were not obvious in *del34* mutants until the later stages of fetal development (Fig. 4D). Histological examination of the *null/null* embryos revealed massive subcutaneous edema (Fig. 4E), which was also present in *del34* embryos but to a lesser degree (data not shown). Anemia and congestive heart failure are major causes of non-immune hydrops fetalis in humans (40,41). However, examination of hemoglobin levels and erythrocyte morphologies as well as serial sections of four *null* and four *del34 Pkd1* homozygous fetal hearts did not show any abnormality (data not shown). Another common cause of hydrops fetalis in humans is skeletal dysplasia (42). Organ-specific targeting of *Pkd1* may elucidate whether the skeletal defects (see below) play a role in the development of hydrops and polyhydramnios in these *Pkd1* mutants. Polyhydramnios may also be exacerbated by obstruction of the gastrointestinal tract due to enlarged cystic pancreas and kidneys at late embryonic stage.

Spina bifida occulta and osteochondrodysplasia in *Pkd1* homozygous mutants

Cartilage and bone develop from multiple embryological origins. The craniofacial skeleton in the first branchial arch and

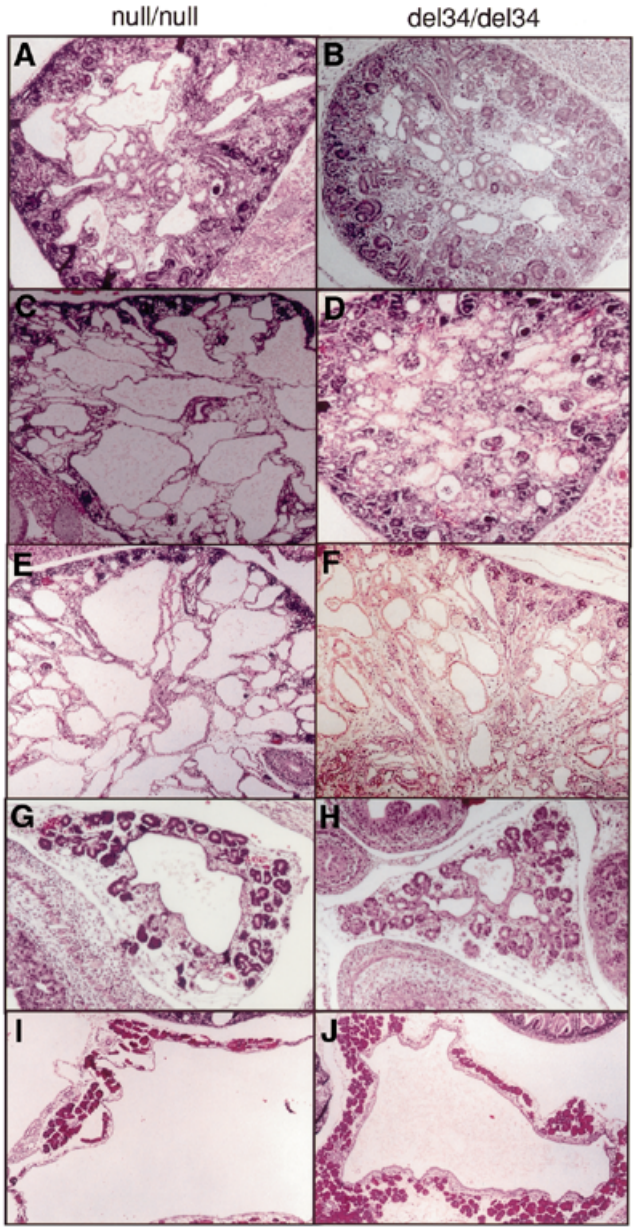

Figure 2. Renal and pancreatic phenotype in *null* and *del34* homozygous kidney. (**A** and **B**) Initial stage of cystic lesions in kidneys at E15.5 in C57BL/6-129 background *null/null* and *del34/del34* mutants (H&E; magnification 50×). Note the severe disease in *null* homozygotes. (**C** and **D**) Cystic kidneys at E17.5 in C57BL/6-129 background in *null/null* and *del34/del34* mutants (H&E; magnification 50×). (**E** and **F**) Cystic kidneys at newborn stage in BALB/c-129 background *null/null* and *del34/del34* mutants (H&E; magnification 50×). Note that the degree of cystic lesion is similar to that in C57BL/6-129 background at E17.5. (**G** and **H**) Pancreatic cysts at E15.5 in C57BL/6-129 background *null/null* and *del34/del34* mutants (H&E; magnification 100×). (**I** and **J**) Pancreatic cysts at E18.5 in BALB/c-129 background *null/null* and *del34/del34* mutants (H&E; magnification 50×).

other regions of the developing head derive largely from neural crest cells. The ribs and vertebrae are from the sclerotomal part of the somites, and the appendicular skeleton is derived from the lateral mesoderm (43). *Pkd1* is expressed at high levels in developing neural tube, neural crest derivatives and prechondrogenic tissue (44). Our *in situ* hybridization studies show that the strongest signals of *Pkd1* were found in the perichondrium of developing vertebrae and long bone (Fig. 5A–G), but absent in the hypertrophic chondrocytes.

To determine whether loss of polycystin-1 in bone has any effects *in vivo*, we looked for skeletal abnormalities in the mutants. Both *null* and *del34* homozygotes developed spina bifida occulta at late embryonic or newborn stages (Fig. 6A). All five *null* homozygotes examined displayed severe defects in vertebral development (Table 3). Non-closure of neural arches started at cervical vertebrae and extended in some cases to sacral vertebrae, with the most severe defects in the lumbar region. The laminae of the lumbar vertebrae were extended; the intact arches remained open and failed to cover the dorsal part of the neural tube (Fig. 6B and E). Eight (73%) of 11 *del34* homozygotes developed mild spina bifida occulta in the lumbar region (Fig. 6C and Table 3). At the newborn stage, the

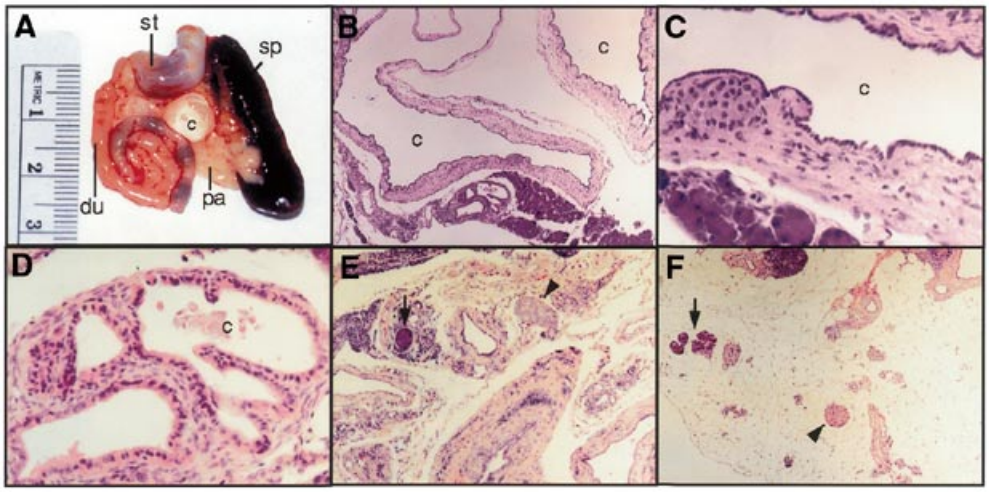

Figure 3. Pancreatic cyst phenotype in a *del34* heterozygote. (**A**) Pancreatic cysts (c) from a 22-month-old *del34* heterozygous mouse. du, duodenum; pa, pancreatic tissue; sp, spleen; st, stomach. (**B**) Multiple pancreatic cysts (c) lined by a monolayer of cuboidal epithelia and thin fibrous wall (H&E; magnification 50×). (**C**) Higher magnification of cyst-lining cuboidal epithelia. Remaining acini can be seen in the lower left corner (H&E; magnification 200×). (**D**) Pancreatic cysts (c) with eosinophilic cuboidal epithelium (H&E; magnification 200×). (**E**) Atrophy of exocrine pancreas with cyst formation, focal fibrosis and adipose replacement. Few acini (arrow) and islets (arrowhead) remain (H&E; magnification 50×). (**F**) In more solid areas, the pancreas is massively replaced by adipose tissue (pancreatic lipomatosis); atrophic acini (arrow) and islets of Langerhans (arrowhead) appear isolated and surrounded by mature adipocytes (H&E; magnification 50×).

Table 3. Newborn $Pkd1^{null/null}$ and $Pkd1^{del34/del34}$ mice with skeletal defects

ID	Genetic background	Spina bifida occulta	Dwarfism	Thyroid cartilage malformation
null/null				
1919-3	BALB/c-129	++	++	++
1968-1	BALB/c-129	++	++	++
1401-2	BALB/c-129	++	++	++
1401-4	BALB/c-129	++	++	++
1401-6	BALB/c-129	++	++	++
del34/del34				
108-1	C57BL/6-129	+	+	–
108-5	C57BL/6-129	–	–	–
108-6	C57BL/6-129	++	++	+
525-1	C57BL/6-129	+	+	–
153-1	BALB/c-129	–	–	–
2512-1	BALB/c-129	++	++	+
201-1	C3H-129	+	+	+
201-3	C3H-129	–	–	–
201-17	C3H-129	+	+	–
201-18	C3H-129	+	++	+
202-1	C3H-129	–	+	–

++, Severe; +, mild; –, negative.

skeletal development in both *del34* and *null* homozygotes was retarded compared with that of wild-type littermates (Fig. 6A and Table 3). There is a delay in bone mineralization of vertebrae, long bones and skull, most obviously in the *null* homozygotes (Fig. 6B–K), although ossification centers remained (Fig. 6E). The thyroid cartilage is malformed in the *null* homozygous mutants (Fig. 6L and Table 3). The long bones in *null* homozygotes were shorter and about a third thinner than those of wild-type animals (Fig. 6G and H). Histology of *null* homozygous long bones shows that the hypertrophic chondrocyte zone is reduced in length at E14.5, similar to what was seen in mice lacking Indian Hedgehog, indicating that loss of polycystin-1 can lead to defective chondrocyte differentiation and maturation. (Fig. 7A–D). At E17.5, bone marrow cavity is formed but shortened (Fig. 7E–H) in the *null* homozygotes. The defective overall ossification of skeletal elements of different origins makes a cell lineage defect as an unlikely cause. This condition is, in fact, reminiscent of human infantile osteodystrophy. These data suggest that polycystin-1 is required for the differentiation of chondrocytes. Its loss leads to defects in the development of the vertebral column, skeletal growth and ossification including intramembranous ossification.

DISCUSSION

Polycystin-1 is required in the final stages of kidney development

To our surprise we observed that some polycystin-1 *null* mutants were able to survive to late gestation, despite high levels of *Pkd1* expression as early as the stem cell stage in development (Lu *et al.*, unpublished data) and the wide distribution of the protein. Furthermore, the *null* kidneys were phenotypically normal until E15.5. Kidney development starts by formation of Wolffian-duct-derived ureteric buds that invade the metanephric mesenchyme at about E11 in the mouse. As a response to bud induction, the mesenchymal cells condense around the ureteric bud. During subsequent branching morphogenesis of the ureteric bud, the condensed mesenchymal cells further proliferate to form pretubular structures that undergo mesenchymal-epithelial transformation to form epithelium-lined tubules and fuse to the branching ureteric bud. These tubules undergo further functional and structural maturation to

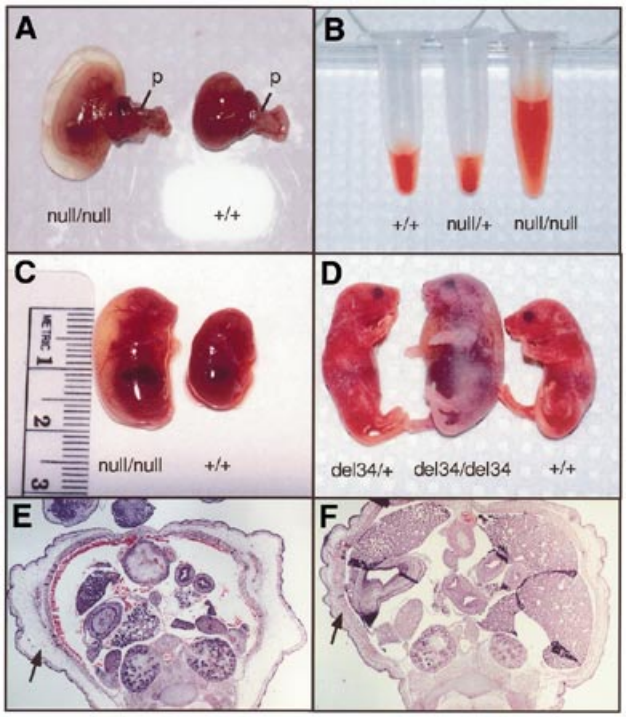

Figure 4. Polyhydroamnios and hydrops in *del34* and *null* homozygotes. (**A**) E14.5 *null* homozygote (*null/null*) and wild-type (+/+) embryos with intact amniotic sac and placenta (p). Excess amniotic fluid was found inside the amniotic sac of the *null* homozygote. (**B**) The amount of amniotic fluid from E14.5 embryos of the same litter with different genotypes. (**C**) Massive systemic edema in an E15.5 *null* homozygote compared with a wild-type littermate. (**D**) Hydrops at a lesser degree was found in *del34* newborn homozygotes (*del34/del34*). Normal heterozygote (*del34*/+) and wild-type (+/+) littermates are shown on either side of the homozygote. (**E**) Massive subcutaneous edema (arrow) in a cross-section of an E15.4 *null* homozygote (H&E; magnification 25×). (**F**) Cross-section of a wild-type littermate of (E) shows normal subcutaneous tissue (arrow) (H&E; magnification 25×).

become fully differentiated tubules in permanent kidneys. This process can be classified into four stages: nephrogenic condensation, epithelialization, initial tubulogenesis and tubular maturation. Our data demonstrate that polycystin-1 is not required in the initial stages of kidney development, although *Pkd1* transcript was strongly expressed in condensing mesenchyme at E12.5 (44). Our data also indicate that a truncated or partially functional polycystin-1 may reduce the rate of cyst formation but not delay the onset of cyst formation, a finding consistent with the previous observation that polycystin-1 expression in the kidney peaks between E15.5 and E18.5, coincident with renal tubule maturation (22–24,45). Thus, the data lend further support for a role of polycystin-1 in terminal differentiation of epithelial cells and maintenance of the structural integrity of renal tubules. Although glomerular expression of polycystin-1 has been reported (33), no obvious abnormality was seen in glomeruli. A similar phenotype has been found in mice with inactivation of the *Pkd2* gene (46).

Loss of polycystin-1 function results in cyst formation in ADPKD

A two-hit hypothesis was proposed as the mechanism of cystogenesis (47) for the sporadic distribution of cysts observed in ADPKD. The hypothesis gained support from the finding of loss of heterozygosity in a small number of cysts (48–50). However, the two-hit theory is contradicted by the findings that polycystin-1 is overexpressed in epithelia from most cysts in kidneys from ADPKD patients (20,21,24,30–33), and that mice overexpressing normal human polycystin-1 develop renal cysts (51).

In this study, we show that homozygous and heterozygous *null* mutants both have phenotypes that are similar to those produced by polycystin-1-overexpressing *del34* mutants (see Results). Two possible conclusions can be drawn from these results: (i) both overexpression and loss of polycystin-1 result in cyst formation and (ii) loss of polycystin-1 leads to cystogenesis. Although overexpression of normal human polycystin-1 in mice does result in cyst formation, these mice have normal fetal development and develop mild glomerular cysts only in late adulthood (51). Moreover, these mice also overexpress a full-length tuberous sclerosis 2 gene whose product is involved in growth control. While it is not clear at the present stage whether polycystin-1 overexpression contributes to cyst formation in ADPKD, the data from our *null* mutants clearly state that loss of polycystin-1 results in cyst formation in *Pkd1* disease.

Although similar, the *null* and *del34* phenotypes are not identical. In homozygotes, the renal tubule and pancreatic duct dilatation was much more rapidly progressive in *null* animals, and at a given age, the number of cysts in homozygotes was greater in *null* than in *del34* mice with the same genetic background. These data provide the first evidence that the nature of the mutation affects disease progression. These data also suggest that a mutant polycystin-1 in *del34* mice partially rescues the phenotype. Indeed, we did detect mutant proteins in *del34* homozygotes by western blotting. The nature of the mutant proteins is currently unknown, but they may be the truncated and/or alternatively read-through or spliced forms of polycystin-1 (52). Although multiple RT–PCRs of the *Pkd1* transcripts of the exon 32–37 region failed to identify alternative spliced transcripts, alternative splicing in other parts of the *Pkd1* gene can not be excluded. On the other hand, the alternative readings of the genetic code, which include leftward and rightward ribosomal frameshifting, programmed termination read-through, and hopping (53,54), may allow the continued translation of mutant *Pkd1* transcripts into near full-length mutant polycystin-1. Nevertheless, our results provide the first evidence of the concurrence of loss-of-function phenotype and increased polycystin-1 expression in *Pkd1* homozygous mutants, thus providing a possible explanation for increased immunoreactive polycystin-1 in ADPKD cyst epithelia in the context of the two-hit model such that the overexpression of polycystin-1 in cysts in ADPKD is due to the detection of mutant polycystin-1 that is unable to function sufficiently. While the germline mutant allele generates increased levels of mutant (e.g. read-through) proteins with little or no function, gradual loss of the second allele due to somatic mutations initiates clonal cyst development in ADPKD.

Polycystin-1 is required for skeletogenesis

Both homozygous *Pkd1*-targeted mutants exhibit osteochondrodysplasia and delayed endochondral and intramembranous bone formation, demonstrating that polycystin-1 is required for

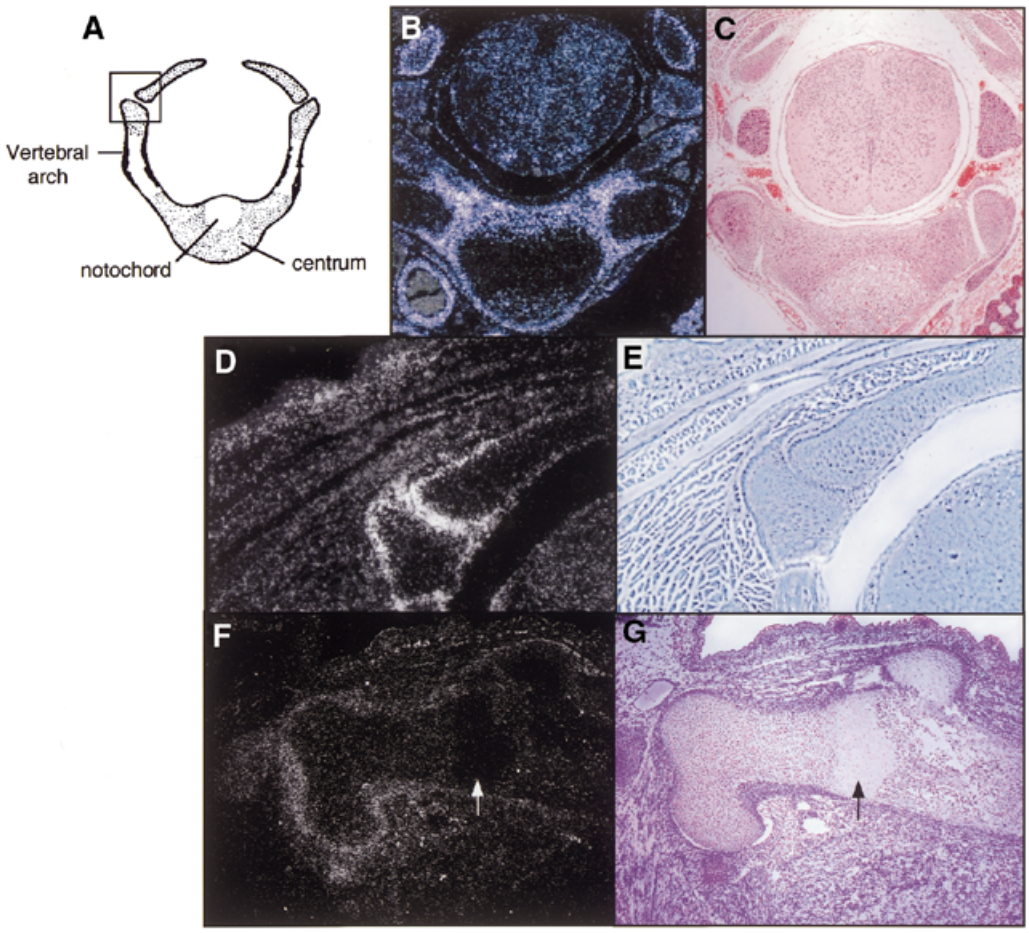

Figure 5. *Pkd1* transcript expression in developing vertebrae and long bone. (**A**) Scheme of lumbar vertebrae in a normal newborn mouse. The enlarged views of the boxed area are in (**D** and **E**). (**B**) Overview of strong expression of *Pkd1* in the lumbar vertebrae (magnification 50×) from a newborn mouse. (**C**) H&E staining of the section adjacent to (B) (magnification 50×). (D) High expression of *Pkd1* in the perichondrium of vertebral arch joint (magnification 100×). (E) Phase contrast of (D) (magnification 100×). (**F**) High expression of *Pkd1* in the perichondrium of distal part of femur from E16.5 embryo. Lower levels of expression can be seen in the resting chondrocytes through prehypertrophic chondrocytes and absent in the hypertrophic chondrocytes (arrow; magnification 50×).(**G**) Toluidine blue staining of the section adjacent to (F) (magnification 50×).

normal mouse skeletogenesis. The function of polycystin-1 in the bone appears to mirror its function in the kidney, such that it is required for chondrocyte differentiation and maturation in the bone, as it is needed for epithelial differentiation and maturation in the kidney. These findings are consistent with polycystin-1 expression patterns in tissues originating from neural crest cells and sclerotic mesenchyme in which polycystin-1 is found at high levels between E12.5 and E17.5.

However, skeletal abnormality is not a general finding in ADPKD patients. The absence of skeletal abnormalities in ADPKD patients may be because of the lack of PKD1 homozygous patients to be assessed, as current study suggests that human PKD1 homozygotes likely die in uterus. In heterozygous patients, depending on the cell type undergoing a somatic hit, and the timing of the second hit, the skeletal phenotype described here may or may not be exhibited. It is noteworthy that several reports have suggested a link between human recessive and possibly dominant polycystic kidney disease and skeletal abnormality (55,56). Our study thus brings up an issue, that if one day we can correct the kidney disease so that homozygous PKD1 patients would survive, the skeletal defects in these children may require medical attention. No significant cardiovascular phenotype and intracranial aneurysm were detected in our mouse models. Whether the lack of these phenotypes is due to the specific mutations we introduced or other factors remains to be investigated.

While study of mouse homozygotes reveals the importance of polycystin-1 in a wider range of tissues than are clinically affected in ADPKD, the phenotype of heterozygous *del34* and *null* mutants largely recapitulate human clinical patterns seen in ADPKD. Thus, our *Pkd1* mutant mouse lines provide excellent models for studies of both the pathogenesis of ADPKD and polycystin functions.

MATERIALS AND METHODS

Generation of *Pkd1 null* mutant mice and breeding scheme

To construct the targeting vector, a P1 clone (clone address, plate 243; control no. 13003, GenomeSystems) containing full-length *Pkd1* genomic DNA was isolated from a 129Sv mouse genomic library. A 6.6 kb *Avr*II-*Nsi*I fragment containing

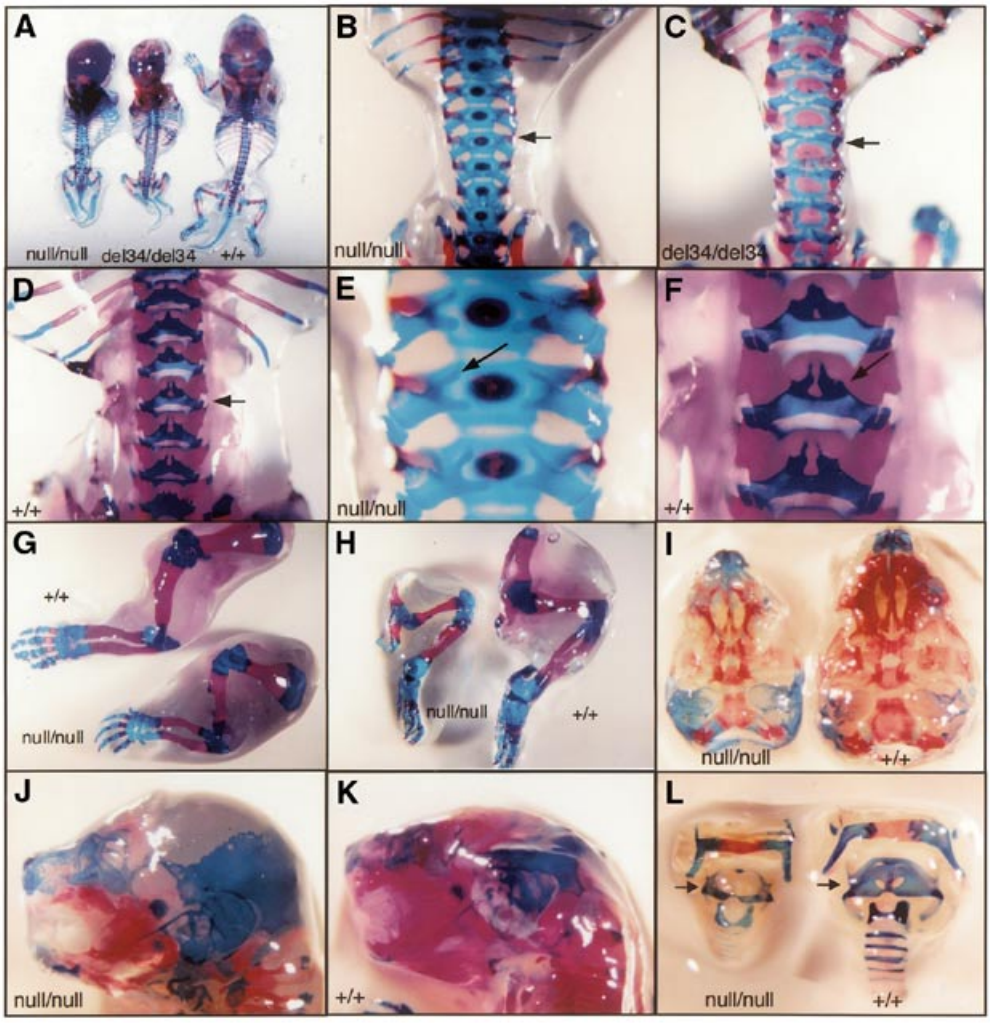

Figure 6. Spinal bifida and osteochondrodysplasia in *Pkd1* homozygous mutants. Newborn mice were stained with alizarin red for bone (red color) and alcian blue for cartilage (blue color), followed by alkaline digestion to allow visualization of the skeleton. Genotypes of the mice are labeled. (**A**) Ventrodorsal view of intact skeletons showing dwarfism and defective ossification in the homozygous mutants. (**B**–**D**) View of lumbar region vertebrae (arrow). Note the wide separation of the neural arches in *null/null*, mild separation in *del34/del34,* and complete closure of neural arches in wild-type (+/+). (**E** and **F**) Close view of *null* homozygous lumbar vertebrae showing the opening of neural arches (arrow) (E) compared with normal wild-type littermate (F). Ossification is initiated but to a lesser degree in the *null* homozygotes. (**G** and **H**) Comparison between forelimbs (G) and hindlimbs (H) of a *null* homozygote and wild-type. (**I**–**K**) The craniofacial skeleton of a newborn *null* homozygote (*null/null*) and its wild-type littermate (+/+); note the delayed mineralization in *null/null*. (**L**) Dorsal view of the laryngeal cartilages; note the defect of the thyroid cartilage (arrow) in mutants.

exons 2–6 was subcloned into vector litmus 28. A phosphoglycerate kinase (*pgk*) promoter-driven neo-resistant selection cassette was inserted into the *PmlI* site of exon 4 in the same orientation. The resulting targeting vector contained 1.1 kb of homologous sequence in the short arm and 5.5 kb in the long arm (Fig. 1A). The targeting vector was electroporated into 129Sv J1 ES cells (a gift from Dr. En Li) and selected according to standard procedures. Positive clones were injected into C57BL/6 and BALB/c blastocysts to generate chimeras.

The chimeras that were derived from C57BL/6 or BALB/c blastocysts were bred with the same inbred strain, respectively. The resulting F_1 heterozygotes were bred with the respective C57BL/6 or BALB/c strain to produce more heterozygotes (N2). Homozygotes were generated by a cross between F_1 heterozygotes or F_1 and N2 heterozygotes. Homozygotes thus contain 129SvJ1 and C57BL/6 genetic components or 129SvJ1 and BALB/c genetic components and are defined as of either C57BL/6-129 or BALB/c-129 background in the text. Heterozygotes and homozygotes were determined by Southern blot of tail and yolk-sac genomic DNA.

Southern blot analysis to genotype ES cells and mice

To identify the targeted mutant ES cells and to genotype the mice, genomic DNA was digested with *Bam*HI and analyzed by Southern blotting. A 1.1 kb *Nae*I fragment (probe 2), which detects a 3.7 kb fragment in wild-type DNA and a 5.4 kb fragment in targeted clones, was used (Fig. 1A and B). A 0.9 kb *Nsi*I-*Avr*II genomic fragment (probe 1) located immediately upstream of the long arm *Avr*II site was used to confirm the homologous recombination in the 5′ homology region. The wild-type *Spe*I fragment detected by this probe is 16 kb, and

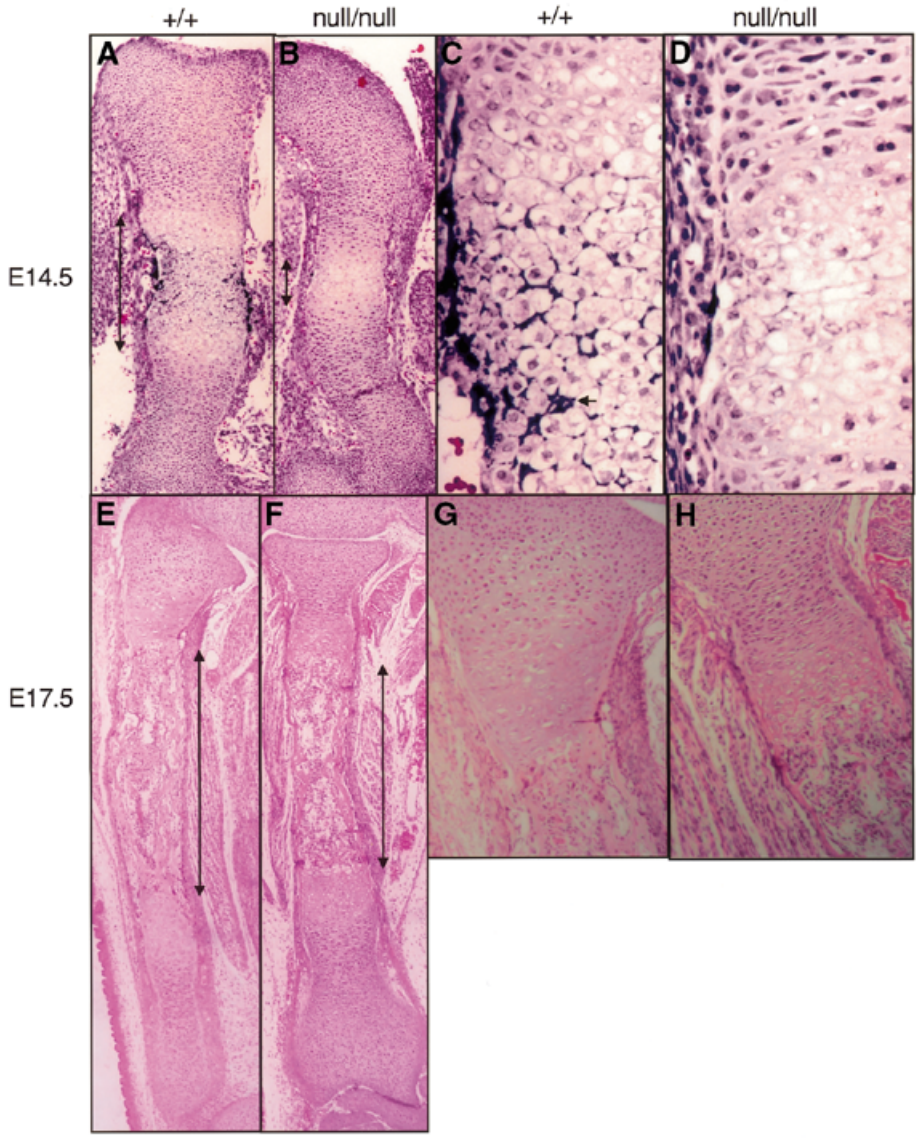

Figure 7. Histological analysis of endochondral ossification in *Pkd1 null/null* mutants. (**A** and **B**) Longitudinal sections of wild-type (+/+) and mutant (*null/null*) humerus from E14.5 embryos. Note the reduced hypertrophic chondrocyte zone in mutant (arrow bar) (H&E; magnification 50×). (**C** and **D**) High magnification of chondrocytes in the center of bones shown in (A and B). Calcium deposits can be easily found in wild-type (arrow), but not in the mutant. (H&E; magnification 50×). (**E** and **F**) Longitudinal sections of wild-type (+/+) and mutant (*null/null*) radius from E17.5 embryos. The bone marrow cavity is formed but slightly reduced (arrow bar) (H&E; magnification 50×) in the mutant. (**G** and **H**) High magnification of proliferating zone of bones shown in (E) and (F) (H&E; magnification 200×).

the mutant fragment is 14.8 kb (data not shown). The homologous recombination frequency was 20%.

Northern blot and RT–PCR analysis

For northern analysis, mRNA was isolated from E12.5 *null* and *del34* whole embryos with a MicroPoly(A)Pure kit (Ambion), separated on 1% agarose/formaldehyde gels, and transferred to BrightStar-Plus positively charged nylon membranes (Ambion). A 1.1 kb mouse cDNA containing *Pkd1* exons 2–6 was used as probes. Hybridization was performed with ExpressHyb hybridization solution (Clontech). Intensity analysis was performed on a Macintosh computer with the public domain NIH image program (developed at the US National Institutes of Health and available on the internet at http://rsb.info.nih.gov/nih-image/).

RT–PCR was carried out with 5 µl total RNA from E16.5 embryos with the SuperScript preamplification system (Life Technologies). Two sets of primers were used (Fig. 1A): set 1, F27 in exon 2 (5′-CTT CAG ACG CTG GAC ATC G-3′)/R37 in exon 5 (5′-GTT GCT TCT ACT TGC ACC TCT G-3′), amplified a 1500 bp fragment in homozygous (*null/null*) RNA and an 800 bp fragment in wild-type (+/+) RNA. Both fragments can be detected in heterozygous (*null*/+) RNA. Set 2, F27 in exon 2/R25 in exon 5 (5′-TAC TGC TGC CAC AGC ACC TG-3′), gives similar results (Fig. 1C). Each mutant transcript was cloned and sequenced by the dideoxy method.

In situ hybridization

Techniques for *in situ* analysis have been described in detail by Sassoon and Rosenthal (57). The probe used for analysis of *Pkd1* was generated from a cDNA fragment corresponding to nucleotide positions 888–1281 (GenBank accession no. U70209) and subcloned into Bluescript SK. Antisense riboprobe was obtained by T7 polymerase with ^{35}S-radiolabeled UTP (>1000 Ci/mmol), following linearization of the plasmid by *Eco*RI to yield a 400-base fragment, and used in a hybridization buffer with an ~35 000 c.p.m./µl final probe concentration.

Antibodies and western blot analysis

Mouse monoclonal antibody 7e12 was raised against an epitope in the N-terminal flank-LRR-flank domain of human polycystin-1 (36).

For western blot analysis, total protein was measured by the Bio-Rad protein assay, ~150 µg/lane of membrane fraction from E12.5 or E16.5 fetal tissue extracts was separated on 5% SDS-polyacrylamide gels at 50 V for 13 h followed by 100 V for 2 h at room temperature. Protein was transferred onto Immobilon-P PVDF membranes (Millipore) at 30 V for 17 h at 4°C in Tris–glycine transfer buffer (Tris 25 mM, glycine 190 mM). The membranes were blocked with 5% non-fat dry milk/TBST and incubated with a monoclonal antibody 7e12 to polycystin-1 at 1:1000. Bound protein was detected by enhanced chemiluminescence (Amersham-Pharmacia).

Histology and skeletal staining

For histological analysis, specimens were fixed in formalin, embedded in paraffin, sectioned at 4 µm, and stained with hematoxylin and eosin (H&E).

Bones and cartilages of completely skinned and freshly eviscerated newborn mice were stained in a mixture of 0.14% alcian blue and 0.12% alizarin red S in ethanol and glacial acetic acid (58) for 2.5 days. Specimens were then macerated in 1.8% KOH for 4 h, cleared in 0.3% KOH overnight and stored in pure glycerin.

ACKNOWLEDGEMENTS

We thank Drs Stephen T.Reeders, Bjorn R.Olsen, Nuria Basora and Mr Eric Williams for discussion, Dr En Li for providing the ES cells, Dr Lin Geng for initial antibody work, Dr Xiaohong Fan for providing mice for skeleton staining, Dr Naomi Fukai for the protocol of skeletal staining and Mr Haidong You for technical assistance. This work was supported by research grants from the National Institutes of Health (NIDDK) to J.Z.

REFERENCES

1. Everson, G.T. (1993) Hepatic cysts in autosomal dominant polycystic kidney disease. *Am. J. Kidney Dis.*, **22**, 520–525.
2. Torra, R., Nicolau, C., Badenas, C., Navarro, S., Perez, L., Estivill, X. and Darnell, A. (1997) Ultrasonographic study of pancreatic cysts in autosomal dominant polycystic kidney disease. *Clin. Nephrol.*, **47**, 19–22.
3. The International Polycystic Kidney Disease Consortium (1994) The polycystic kidney disease 1 gene encodes a 14 kb transcript and lies within a duplicated region on chromosome 16. The European Polycystic Kidney Disease Consortium [Errata (1994) *Cell*, **78**, 4 and (1995) *Cell*, **81**, 7]. *Cell*, **77**, 881–894.
4. The International Polycystic Kidney Disease Consortium (1995) Polycystic kidney disease: the complete structure of the PKD1 gene and its protein. The International Polycystic Kidney Disease Consortium. *Cell*, **81**, 289–298.
5. Burn, T.C., Connors, T.D., Dackowski, W.R., Petry, L.R., Van Raay, T.J., Millholland, J.M., Venet, M., Miller, G., Hakim, R.M., Landes, G.M. *et al.* (1995) Analysis of the genomic sequence for the autosomal dominant polycystic kidney disease (PKD1) gene predicts the presence of a leucine-rich repeat. The American PKD1 Consortium (APKD1 Consortium). *Hum. Mol. Genet.*, **4**, 575–582.
6. Hughes, J., Ward, C.J., Peral, B., Aspinwall, R., Clark, K., San Millan, J.L., Gamble, V. and Harris, P.C. (1995) The polycystic kidney disease 1 (PKD1) gene encodes a novel protein with multiple cell recognition domains. *Nat. Genet.*, **10**, 151–160.
7. Mochizuki, T., Wu, G., Hayashi, T., Xenophontos, S.L., Veldhuisen, B., Saris, J.J., Reynolds, D.M., Cai, Y., Gabow, P.A., Pierides, A. *et al.* (1996) PKD2, a gene for polycystic kidney disease that encodes an integral membrane protein. *Science*, **272**, 1339–1342.
8. Qian, F., Germino, F.J., Cai, Y., Zhang, X., Somlo, S. and Germino, G.G. (1997) PKD1 interacts with PKD2 through a probable coiled-coil domain. *Nat. Genet.*, **16**, 179–183.
9. Tsiokas, L., Kim, E., Arnould, T., Sukhatme, V.P. and Walz, G. (1997) Homo- and heterodimeric interactions between the gene products of PKD1 and PKD2. *Proc. Natl Acad. Sci. USA*, **94**, 6965–6970.
10. Parnell, S.C., Magenheimer, B.S., Maser, R.L., Rankin, C.A., Smine, A., Okamoto, T. and Calvet, J.P. (1998) The polycystic kidney disease-1 protein, polycystin-1, binds and activates heterotrimeric G-proteins *in vitro*. *Biochem. Biophys. Res. Commun.*, **251**, 625–631.
11. Kim, E., Arnould, T., Sellin, L., Benzing, T., Comella, N., Kocher, O., Tsiokas, L., Sukhatme, V.P. and Walz, G. (1999) Interaction between RGS7 and polycystin. *Proc. Natl Acad. Sci. USA*, **96**, 6371–6376.
12. Nomura, H., Turco, A.E., Pei, Y., Kalaydjieva, L., Schiavello, T., Weremowicz, S., Ji, W., Morton, C.C., Meisler, M., Reeders, S.T. *et al.* (1998) Identification of PKDL, a novel polycystic kidney disease 2-like gene whose murine homologue is deleted in mice with kidney and retinal defects. *J. Biol. Chem.*, **273**, 25967–25973.
13. Hughes, J., Ward, C.J., Aspinwall, R., Butler, R. and Harris, P.C. (1999) Identification of a human homologue of the sea urchin receptor for egg jelly: a polycystic kidney disease-like protein. *Hum. Mol. Genet.*, **8**, 543–549.
14. Guo, L., Schreiber, T.H., Weremowicz, S., Morton, C.C., Lee, C. and Zhou, J. (2000) Identification and characterization of a novel polycystin family member, polycystin-L2, in mouse and human: sequence, expression, alternative splicing, and chromosomal localization. *Genomics*, **64**, 241–251.
15. Chen, X.Z., Vassilev, P.M., Basora, N., Peng, J.B., Nomura, H., Segal, Y., Brown, E.M., Reeders, S.T., Hediger, M.A. and Zhou, J. (1999) Polycystin-L is a calcium-regulated cation channel permeable to calcium ions. *Nature*, **401**, 383–386.
16. Hanaoka, K., Qian, F., Boletta, A., Bhunia, A.K., Piontek, K., Tsiokas, L., Sukhatme, V.P., Guggino, W.B. and Germino, G.G. (2000) Co-assembly of polycystin-1 and -2 produces unique cation-permeable currents. *Nature*, **408**, 990–994.
17. Gonzalez-Perret, S., Kim, K., Ibarra, C., Damiano, A.E., Zotta, E., Batelli, M., Harris, P.C., Reisin, I.L., Arnaout, M.A. and Cantiello, H.F. (2001) Polycystin-2, the protein mutated in autosomal dominant polycystic kidney disease (ADPKD), is a Ca^{2+}-permeable nonselective cation channel. *Proc. Natl Acad. Sci. USA*, **98**, 1182–1187.
18. Vassilev, P., Guo, L., Chen, X.Z., Segal, Y., Peng, J.B., Basora, N., Babakhanlou, H., Cruger, G., Kanazirska, M., Ye, C.P. *et al.* (2001) Polycystic kidney disease 2 gene encodes a novel high conductance channel implicated in defective intracellular Ca^{2+} homeostasis. *Biochem. Biophys. Res. Commun.*, **282**, 341–350.
19. Chen, X.Z., Segal, Y., Basora, N., Guo, L., Peng, J.B., Babakhanlou, H., Vassilev, P.M., Brown, E.M., Hediger, M.A. and Zhou, J. (2001) Transport function of the naturally occurring pathogenic polycystin-2 mutant, R742X. *Biochem. Biophys. Res. Commun.*, **282**, 1251–1256.
20. Ward, C.J., Turley, H., Ong, A.C., Comley, M., Biddolph, S., Chetty, R., Ratcliffe, P.J., Gattner, K. and Harris, P.C. (1996) Polycystin, the polycystic kidney disease 1 protein, is expressed by epithelial cells in fetal, adult, and polycystic kidney. *Proc. Natl Acad. Sci. USA*, **93**, 1524–1528.
21. Geng, L., Segal, Y., Peissel, B., Deng, N., Pei, Y., Carone, F., Rennke, H.G., Glucksmann-Kuis, A.M., Schneider, M.C., Ericsson, M. *et al.* (1996)

Identification and localization of polycystin, the PKD1 gene product. *J. Clin. Invest.*, **98**, 2674–2682.
22. Geng, L., Segal, Y., Pavlova, A., Barros, E.J., Lohning, C., Lu, W., Nigam, S.K., Frischauf, A.M., Reeders, S.T. and Zhou, J. (1997) Distribution and developmentally regulated expression of murine polycystin. *Am. J. Physiol.*, **272**, F451–F459.
23. Ibraghimov-Beskrovnaya, O., Dackowski, W.R., Foggensteiner, L., Coleman, N., Thiru, S., Petry, L.R., Burn, T.C., Connors, T.D., Van Raay, T., Bradley, J. *et al.* (1997) Polycystin: *in vitro* synthesis, *in vivo* tissue expression, and subcellular localization identifies a large membrane-associated protein. *Proc. Natl Acad. Sci. USA*, **94**, 6397–6402.
24. Van Adelsberg, J., Chamberlain, S. and D'Agati, V. (1997) Polycystin expression is temporally and spatially regulated during renal development. *Am. J. Physiol.*, **272**, F602–F609.
25. Lu, W., Peissel, B., Babakhanlou, H., Pavlova, A., Geng, L., Fan, X., Larson, C., Brent, G. and Zhou, J. (1997) Perinatal lethality with kidney and pancreas defects in mice with a targetted Pkd1 mutation. *Nat. Genet.*, **17**, 179–181.
26. Lu, W., Fan, X., Basora, N., Babakhanlou, H., Law, T., Rifai, N., Harris, P., Perez-Atayde, A., Rennke, H. and Zhou, J. (1999) Late onset of renal and hepatic cysts in Pkd1-targeted heterozygotes. *Nat. Genet.*, **21**, 160–161.
27. Peral, B., San Millan, J.L., Ong, A.C., Gamble, V., Ward, C.J., Strong, C. and Harris, P.C. (1996) Screening the 3′ region of the polycystic kidney disease 1 (PKD1) gene reveals six novel mutations. *Am. J. Hum. Genet.*, **58**, 86–96.
28. Daniells, C., Maheshwar, M., Lazarou, L., Davies, F., Coles, G. and Ravine, D. (1998) Novel and recurrent mutations in the PKD1 (polycystic kidney disease) gene. *Hum. Genet.*, **102**, 216–220.
29. Badenas, C., Torra, R., San Millan, J.L., Lucero, L., Mila, M., Estivill, X. and Darnell, A. (1999) Mutational analysis within the 3′ region of the PKD1 gene. *Kidney Int.*, **55**, 1225–1233.
30. Harris, P.C. and Watson, M.L. (1997) Autosomal dominant polycystic kidney disease: neoplasia in disguise? *Nephrol. Dial. Transplant.*, **12**, 1089–1090.
31. Ong, A.C. and Harris, P.C. (1997) Molecular basis of renal cyst formation–one hit or two? *Lancet*, **349**, 1039–1040.
32. Ong, A.C., Ward, C.J., Butler, R.J., Biddolph, S., Bowker, C., Torra, R., Pei, Y. and Harris, P.C. (1999) Coordinate expression of the autosomal dominant polycystic kidney disease proteins, polycystin-2 and polycystin-1, in normal and cystic tissue. *Am. J. Pathol.*, **154**, 1721–1729.
33. Peters, D.J., Spruit, L., Klingel, R., Prins, F., Baelde, H.J., Giordano, P.C., Bernini, L.F., de Heer, E., Breuning, M.H. and Bruijn, J.A. (1996) Adult, fetal, and polycystic kidney expression of polycystin, the polycystic kidney disease-1 gene product. *Lab. Invest.*, **75**, 221–230.
34. Brook-Carter, P.T., Peral, B., Ward, C.J., Thompson, P., Hughes, J., Maheshwar, M.M., Nellist, M., Gamble, V., Harris, P.C. and Sampson, J.R. (1994) Deletion of the TSC2 and PKD1 genes associated with severe infantile polycystic kidney disease–a contiguous gene syndrome. *Nat. Genet.*, **8**, 328–332.
35. Sampson, J.R., Maheshwar, M.M., Aspinwall, R., Thompson, P., Cheadle, J.P., Ravine, D., Roy, S., Haan, E., Bernstein, J. and Harris, P.C. (1997) Renal cystic disease in tuberous sclerosis: role of the polycystic kidney disease 1 gene. *Am. J. Hum. Genet.*, **61**, 843–851.
36. Ong, A.C., Harris, P.C., Davies, D.R., Pritchard, L., Rossetti, S., Biddolph, S., Vaux, D.J., Migone, N. and Ward, C.J. (1999) Polycystin-1 expression in PKD1, early-onset PKD1, and TSC2/PKD1 cystic tissue. *Kidney Int.*, **56**, 1324–1333.
37. Oppenheimer, E.H. and Esterly, J.R. (1975) Pathology of cystic fibrosis review of the literature and comparison with 146 autopsied cases. *Perspect. Pediatr. Pathol.*, **2**, 241–278.
38. Andersen, H.M., Drew, J.H., Beischer, N.A., Hutchison, A.A. and Fortune, D.W. (1983) Non-immune hydrops fetalis: changing contribution to perinatal mortality. *Br. J. Obstet. Gynecol.*, **90**, 636–639.
39. Hutchison, A.A., Drew, J.H., Yu, V.Y., Williams, M.L., Fortune, D.W. and Beischer, N.A. (1982) Nonimmunologic hydrops fetalis: a review of 61 cases. *Obstet. Gynecol.*, **59**, 347–352.
40. Arcasoy, M.O. and Gallagher, P.G. (1995) Hematologic disorders and nonimmune hydrops fetalis. *Semin. Perinatol.*, **19**, 502–515.
41. Apkon, M. (1995) Pathophysiology of hydrops fetalis. *Semin. Perinatol.*, **19**, 437–446.
42. Van Maldergem, L., Jauniaux, E., Fourneau, C. and Gillerot, Y. (1992) Genetic causes of hydrops fetalis. *Pediatrics*, **89**, 81–86.
43. Karsenty, G. (1998) Genetics of skeletogenesis. *Dev. Genet.*, **22**, 301–313.
44. Guillaume, R., D'Agati, V., Daoust, M. and Trudel, M. (1999) Murine Pkd1 is a developmentally regulated gene from morula to adulthood: role in tissue condensation and patterning. *Dev. Dyn.*, **214**, 337–348.
45. Griffin, M.D., Torres, V.E., Grande, J.P. and Kumar, R. (1996) Immunolocalization of polycystin in human tissues and cultured cells. *Proc. Assoc. Am. Physicians*, **108**, 185–197.
46. Wu, G., Markowitz, G.S., Li, L., D'Agati, V.D., Factor, S.M., Geng, L., Tibara, S., Tuchman, J., Cai, Y., Park, J.H. *et al.* (2000) Cardiac defects and renal failure in mice with targeted mutations in Pkd2. *Nat. Genet.*, **24**, 75–78.
47. Reeders, S.T. (1992) Multilocus polycystic disease. *Nat. Genet.*, **1**, 235–237.
48. Qian, F., Watnick, T.J., Onuchic, L.F. and Germino, G.G. (1996) The molecular basis of focal cyst formation in human autosomal dominant polycystic kidney disease type I. *Cell*, **87**, 979–987.
49. Brasier, J.L. and Henske, E.P. (1997) Loss of the polycystic kidney disease (PKD1) region of chromosome 16p13 in renal cyst cells supports a loss-of-function model for cyst pathogenesis. *J. Clin. Invest.*, **99**, 194–199.
50. Qian, F. and Germino, G.G. (1997) 'Mistakes happen': somatic mutation and disease. *Am. J. Hum. Genet.*, **61**, 1000–1005.
51. Pritchard, L., Sloane-Stanley, J.A., Sharpe, J.A., Aspinwall, R., Lu, W., Buckle, V., Strmecki, L., Walker, D., Ward, C.J., Alpers, C.E. *et al.* (2000) A human PKD1 transgene generates functional polycystin-1 in mice and is associated with a cystic phenotype. *Hum. Mol. Genet.*, **9**, 2617–2627.
52. Farabaugh, P.J. (1993) Alternative readings of the genetic code. *Cell*, **74**, 591–596.
53. Atkins, J.F., Weiss, R.B. and Gesteland, R.F. (1990) Ribosome gymnastics–degree of difficulty 9.5, style 10.0. *Cell*, **62**, 413–423.
54. Weiss, R.B. (1991) Ribosomal frameshifting, jumping and readthrough. *Curr. Opin. Cell Biol.*, **3**, 1051–1055.
55. Hallermann, C., Mucher, G., Kohlschmidt, N., Wellek, B., Schumacher, R., Bahlmann, F., Shahidi-Asl, P., Theile, U., Rudnik-Schoneborn, S., Muntefering, H. *et al.* (2000) Syndrome of autosomal recessive polycystic kidneys with skeletal and facial anomalies is not linked to the ARPKD gene locus on chromosome 6p. *Am. J. Med. Genet.*, **90**, 115–119.
56. Turco, A.E., Padovani, E.M., Chiaffoni, G.P., Peissel, B., Rossetti, S., Marcolongo, A., Gammaro, L., Maschio, G. and Pignatti, P.F. (1993) Molecular genetic diagnosis of autosomal dominant polycystic kidney disease in a newborn with bilateral cystic kidneys detected prenatally and multiple skeletal malformations. *J. Med. Genet.*, **30**, 419–422.
57. Sassoon, D. and Rosenthal, N. (1993) Detection of messenger RNA by *in situ* hybridization. *Methods Enzymol.*, **225**, 384–404.
58. Kimmel, C.A. and Trammell, C. (1981) A rapid procedure for routine double staining of cartilage and bone in fetal and adult animals. *Stain Technol.*, **56**, 271–273.